

A MODEL FOR THE FAST IONIC DIFFUSION IN ALUMINA-
DOPED LiI

A.M. Stoneham[†], Evelyn Wade^{†*} and J.A. Kilner^{**}

[†]Theoretical Physics Division, AERE Harwell, Didcot, Oxon OX11 0RA

^{*}On attachment from the School of Mathematics, University of Bath

^{**}Department of Ceramics, Houldsworth School of Applied Science
University of Leeds.

(Received March 12, 1979; Communicated by J. B. Goodenough)

ABSTRACT Lithium Iodide shows enhanced ionic conductivity when doped with a powder of the insulator, alumina. We extend Landauer's effective medium model to see if the observations are consistent with a high conductivity layer forming on each non-conducting particle. The predictions are consistent with experiment provided one assumes the layer a few hundred Angstroms thick. At the outside, away from the particle, the enhancement of conductivity should fall off slowly, as in Debye-Huckel screening, whereas it is possible a new phase forms close to the insulator surface.

1. Introduction

Lithium iodide is an ionic crystal with a very modest ionic conductivity. Aluminium oxide is an ionic insulator with an exceedingly small conductivity. It is thus a matter of some surprise to learn that LiI doped with powdered Al_2O_3 has a very high ionic conductivity (1-3). The precise reasons are not established. However, it is reasonable to suggest a model in which each alumina particle is surrounded by an interfacial layer of characteristic thickness t and with a high conductivity which falls to the usual LiI value at large distances. This paper examines the expected ionic conductivity in this model, and verifies that it gives a satisfactory description of what is observed.

The precise nature of the boundary layer is not important provided we can estimate its characteristic thickness and conductivity. Several explanations of the layer are possible. It could be that the LiI- Al_2O_3 interface

encourages the formation of intrinsic defects in its neighbourhood, for example by acting as a sink for Li interstitials. Alternatively, the hexagonal form of LiI might form locally and have a higher conductivity. Owens & Hanson (3) suggest that water is involved. LiI is notoriously hygroscopic, and the monohydrate, $\text{LiI}\cdot\text{H}_2\text{O}$, seems a suitable candidate for the interfacial layer.

2. Conductivity: The Average Medium Model

We follow here the analysis of Landauer (4) in his analysis of the conductivity of a random mixture of two media in good electrical contact and with differing conductivities. Our description differs from that of Landauer because of the nature of the system under discussion, but is similar in spirit. Other workers (5,6) have reviewed developments since Landauer's paper and there has also been application to lithium ion conduction in glasses (7).

The essence of Landauer's approach is this. If the two media are labelled 1 and 2, one considers in turn the polarisation of a sphere of each in an average medium. The average medium itself is then taken to have the consistently-chosen conductivity appropriate to the aggregate of the two components. The conductivity of this aggregate then follows directly. In our case, the problem is somewhat more complicated. It is clear that LiI, far from any Al_2O_3 , should constitute one of the media. It is equally clear that the model of the other component should recognise that the highly-conducting boundary layer lies on a non-conducting core. There are thus several generalisations. We must consider a structured sphere (fig. 1)

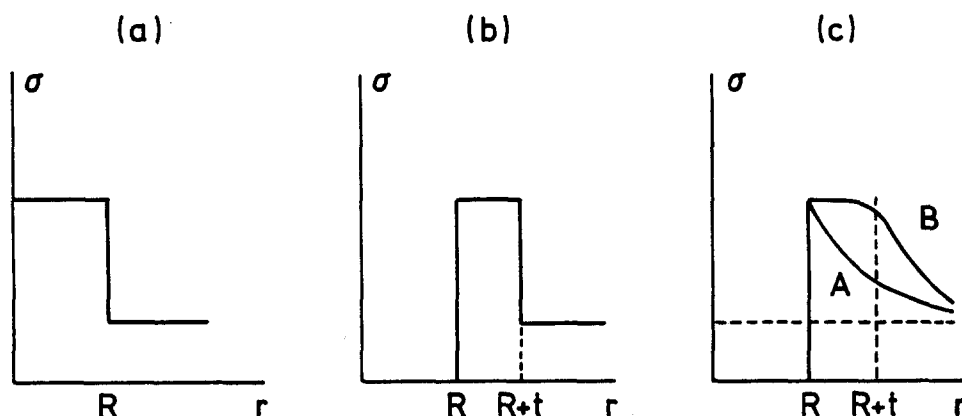


FIG. 1.

FIG. 1 Spatial distribution of conductivity near an alumina particle of radius R in LiI

- (a) Landauer model
- (b) Discrete shell model. This assumes Al_2O_3 does not conduct, and that the conductivity at large distances is that of pure LiI.
- (c) Screening layer model: the conductivity changes continuously, rather than abruptly. The characteristic length is probably a few hundred Angstroms, comparable with typical Debye-Hückel radii.

when we calculate the polarisation of the alumina plus boundary layer. We must also ask whether the non-conducting alumina blocks ionic conduction appreciably at high doping levels, and how we should count the contributions from those regions which are close to more than one alumina particle.

The present calculations are based on the discrete shell model of figure (1b), though we shall discuss the different implications of (1c) too. The generalisation of Landauer's work is straightforward, though it is too complicated to quote in full. In essence, the complications appear because one needs the complex susceptibility of a system in which the basic units are no longer uniform spheres. The main result is that the effective conductivity of the average medium can be obtained from the imaginary part of k_{av} :

$$k_{av} = \beta + \sqrt{\beta^2 + \gamma}$$

in which the variables are:

$$\beta = [k_1(1-2Y)(2-\theta) - k_L(1-Y)(1-2\theta)]/4(1+Y)(1+\theta)$$

$$\gamma = k_1 k_L (1-2Y)/4(1+Y).$$

The dielectric constants are k_0 for Al_2O_3 and k_1 for the boundary layer. If the Al_2O_3 particle radius is R and the boundary layer thickness is t , then $Y \equiv [R^3/(R+t)^3](k_1-k_0)/(2k_1+k_0)$. The volume fraction of Al_2O_3 is x_0 , and defines θ through

$$x_0 \equiv [R^3/(R+t)^3]/(\theta+1).$$

In these expressions we have used the average medium theory for the complex susceptibility, rather than just the conductivity component. There are thus some differences from Kerner's results (8); these differences are negligible at low doping, and they do not affect our conclusions. The limits for extreme values of t and with special cases of k_1 agree with Landauer's result. Very similar expressions can be derived for more general models with several layers to give an approximation to the system shown in fig. (1c). It will be noticed that the expressions for k_{av} depend only on t/R and on the volume fraction of alumina. There is no explicit dependence on R separately, though there is an implicit assumption that t/R is the same in all cases when there is a dispersion of particle sizes.

Figure 2 shows the results of calculations of the conductivity in the low frequency regime (the results are indistinguishable for frequencies from 0.1 to 10 Hertz). For simplicity, the real part of the dielectric constants of Al_2O_3 , LiI and the boundary layer have been taken as 11.0, reasonably close to the known values. The conductivity of LiI was taken as $10^{-7} \Omega^{-1} \text{cm}^{-1}$ (ref (1)) and that of the boundary layer as $3.5 \cdot 10^{-5} \Omega^{-1} \text{cm}^{-1}$ from the highest conductivities quoted in ref. (3).

The results show quite good accord with experiment for boundary-layer thicknesses of 30-50% of the alumina particle radii. Owens & Hanson (3) discuss alumina powders of $85 \text{ m}^2/\text{gm}$ surface area, corresponding to radii of about 1400 \AA . The thicknesses deduced are around 500 \AA , somewhat larger than the Debye-Hückel screening length, but consistent with a picture of locally-enhanced defect concentrations. There are, however, two glaring discrepancies in Figure 2. First, the conductivity falls off less rapidly than predicted

FIG. 2 Simple theory of the conductivity using the model of figure (1b). The conductivity is in units $10^{-6} \Omega^{-1} \text{cm}^{-1}$ as a function of the molar percentage of Al_2O_3 . The numbers on the curves are $(R+t)/R$. The dotted line through the experimental points is merely to guide the eye. The conductivity of the boundary layer corresponds to $\sigma=35$ in the units used and is presumably an upper bound.

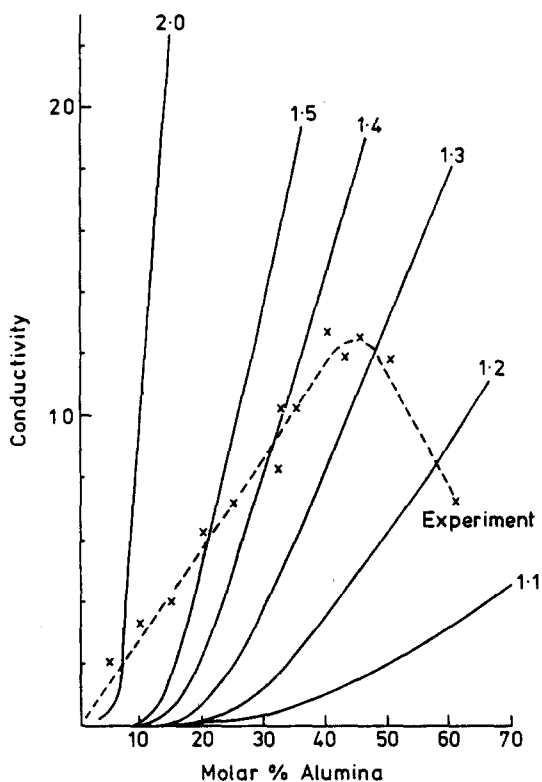


FIG. 2.

at low alumina levels. Secondly, the conductivity is observed to fall when the alumina content becomes large. We shall return to the high-concentration limit in the next section. The low-concentration discrepancy suggests an important point: the spatial distribution of conductivity must resemble that of Fig. (1c) rather than Fig. (1b). Even at low concentration, the tails of enhanced conductivity can overlap and give a more rapid effective bulk conductivity.

3. Limits to the Conductivity at high doping levels

Broadly, two factors might contribute to the fall-off in conductivity at higher alumina contents. The first can be described as "blocking". Alumina itself is essentially non-conducting. If a fraction f of the area of a plane through the electrolyte consists of alumina, only a fraction $(1-f)$ is free to conduct ions, irrespective of any enhancement near an alumina particle. The second can be described as "saturation". Suppose the local enhancement of the conductivity is caused by the appearance of a new phase, possibly $\text{LiI}\cdot\text{H}_2\text{O}$. The conductivity of this phase will be the same whether it has one, two, three or more particles adjacent to it: the extra particles have no effect. If, however, each particle caused an extra increment in the defect concentrations, the behaviour would be different. Suppose the fraction of the total volume

within t of one particle is ϕ_1 , that within t of two particles ϕ_2 , etc. Then the total volume of a new distinct phase would be the fraction $\phi_1 - \frac{1}{2}\phi_2 - \frac{2}{3}\phi_3 - \dots - \frac{N-1}{N}\phi_N \dots$, rather than just ϕ_1 .

It is far from trivial to calculate the precise form of the limit, especially since geometric models do not mix easily with average medium arguments. What one can do is to list $(1-f)$ and $(\phi_1 - \sum_{N=2}^{\infty} \frac{N-1}{N} \phi_N)/\phi_1$ as rough and ready correction factors, and note the situations in which they become important.

FIG. 3 Full lines indicate saturation effects from the overlap of boundary layers for various values of $(R+t)/R$. The broken line is $(1-f)$ and approximates the effects of blocking.

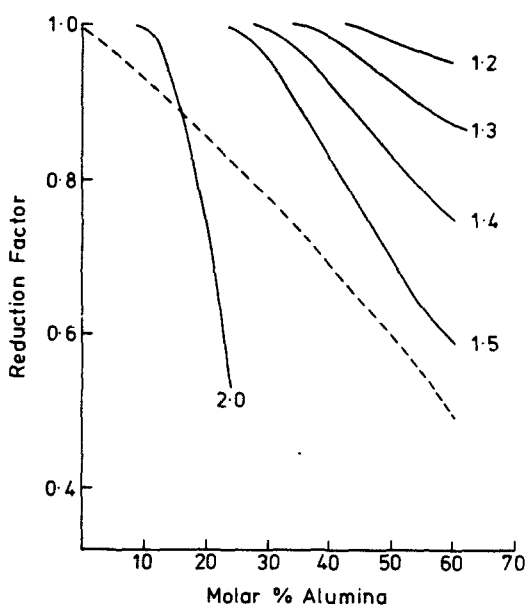


FIG. 3.

The results are shown in Fig. 3. Even these simple results indicate two features. One is that blocking simply produces a smooth trend which does not correspond to the experimental results given in Fig. 2. Saturation, however, begins to become important at the observed level of alumina doping for exactly the value of t/R deduced from figure 2.

4. Conclusions

Combining the analyses of the low concentration and high concentration data, the conclusions of our calculations are these. First, the data can be fitted assuming a lithium-ion conducting boundary layer around each alumina particle. Secondly, the low-alumina results imply the conducting region does not end abruptly, but tails off into the bulk. Thirdly, the high alumina results show the conductivity has reached a saturation value close to the alumina particle. The results are all consistent with a thickness t for the boundary in the sense of Fig. 1(c), curve B.

The results suggest that the highest ionic conductivity will be reached with very fine alumina powder, so that blockage is minimised. If the thickness t of the boundary layer is roughly constant down to the very smallest radii R , the maximum conductivity corresponds to that of the boundary layer itself. With $t = 500 \text{ \AA}$ and $R \ll t$, around $2 \cdot 10^{-9}$ alumina particles per cc could give the maximum conductivity of $3.5 \cdot 10^{-6} \Omega^{-1} \text{ cm}^{-1}$ assumed in §2. Clearly, one might imagine that the alumina particles less than some critical radius R_c are less effective. Nevertheless, enhancement to near the maximum should be possible provided the particles are as small as possible consistent with R_c . The gains which might be achieved are useful, rather than dramatic; the maximum observed conductivity shown in Fig. 2 is around $13 \cdot 10^{-6} \Omega^{-1} \text{ cm}^{-1}$, so that a factor 2-3 improvement is the most one might expect.

1. C.C. Liang 1973 U.S. Patent 3541 124
1973 J. Electrochem Soc 120 1289
2. C.C. Liang & L.H. Barinette 1976 J Electrochem Soc 123 453
3. B.B. Owens & H.J. Hanson 1977 U.S. Patent 4007122
4. R. Landauer 1952 J Appl Phys 23 779
5. S. Kirkpatrick 1973 Rev Mod Phys 45 574
6. D. T. Bergmann 1978 Physics Reports 43(9)
7. R.M. Biefeld, G.E. Pike & R.T. Johnson 1977 Phys Rev B15, 5912
8. E.R. Kerner 1956 Proc Phys Soc B69 808